Online version at http://www.minervamedica.it

The Quarterly Journal of Nuclear Medicine and Molecular Imaging 2021 March;65(1):72-8
DOI: 10.23736/S1824-4785.19.03137-6

ORIGINAL ARTICLE

Differential diagnostic ability of ^{18}F-FDG PET/CT radiomics features between renal cell carcinoma and renal lymphoma

Sha ZHU [1, 2], Hui XU [3], Chuyu SHEN [2], Yingjie WANG [2], Wenting XU [2], Shihao DUAN [2], Hanxiao CHEN [2], Xuejin OU [2], Linyan CHEN [2], Xuelei MA [4] *

[1]Department of Urology, West China Hospital, Sichuan University, Chengdu, China; [2]West China School of Medicine, West China Hospital, Sichuan University, Chengdu, China; [3]Department of Radiology, West China Hospital, Sichuan University, Chengdu, China; [4]National Collaborative Innovation Center for Biotherapy, West China Hospital, Sichuan University, Chengdu, China

*Corresponding author: Xuelei Ma, West China Hospital, 37 Guoxue Xiang, Chengdu 610041, Sichuan, China. E-mail: drmaxuelei@gmail.com

ABSTRACT

BACKGROUND: The aim of this study is to determine the differential diagnostic value of texture parameters of PET/CT on renal cell carcinoma and renal lymphoma.

METHODS: Twenty renal lymphoma and 18 renal cell carcinoma (RCC) patients were analyzed in this study. The pathological information and basic characteristics were extracted from the electronic medical record system of our hospital. We used LIFEx package to extract data from the radiomics images. Receiver operating characteristic analysis and binary logistic regression analysis was applied in determining the diagnostic accuracy of texture parameters as well as the synthetic parameter, of which the sensitivity and specificity was improved.

RESULTS: There were 14 (two in Histogram, two in Grey Level Co-occurrence Matrix, five in Grey-Level Run Length Matrix, five in Grey-Level Zone Length Matrix) out of the texture parameters showing an area under the curve (AUC) >0.7 and P<0.05. Synthesized parameters of each section showed even higher differentiation ability, with AUC varying from 0.725 to 1.000.

CONCLUSIONS: Texture analysis of ^{18}F-FDG PET/CT could effectively differentiate between RCCs and renal lymphomas.

(*Cite this article as:* Zhu S, Xu H, Shen C, Wang Y, Xu W, Duan S, *et al*. Differential diagnostic ability of ^{18}F-FDG PET/CT radiomics features between renal cell carcinoma and renal lymphoma. Q J Nucl Med Mol Imaging 2021;65:72-8. DOI: 10.23736/S1824-4785.19.03137-6)

KEY WORDS: Renal cell carcinoma; Lymphoma; Differential diagnosis.

Due to the pervasive application of abdominal imaging examinations, renal masses are more frequently found by accident. Renal masses are a histologically heterogeneous group ranging from benign lesions to malignant tumors,[1] the treatment of which also varies according to different pathological nature of the masses.[2] Consequently, the discrimination of the renal masses through non-invasive methods like imaging process is pivotal during clinical management.

Renal cell carcinoma (RCC) is the most common type of renal malignancies in adults.[3] Surgical resection, radical or partial, is considered the most reliable way to achieve curative outcome for localized RCC patients.[4, 5] Meanwhile, lymphoma is defined as a hematologic malignancy derived from lymphoid cells. But it is not confined to lymphoid tissue, though, since the involvement of extra-nodular sites such as kidney is occasionally seen. Systemic chemotherapy and radiotherapy are commonly applied in treating these patients, as well as other options like stem cell transplantation.[6-8] Although non-Hodgkin lymphoma with kidney involvement is not common during clinical work, it is still found in autopsy in about 34 percent of patients and often causes misdiagnosis by masquerading as RCC or other diseases.[9-11] In view of the radical difference lying in the treatment algorithms between RCC and renal lymphoma, it is of significance to differentiate these two pathological types.

Texture analysis (TA) is being heatedly discussed recently, especially in the imaging diagnosis and prognosis prediction area.[12] In simple terms, TA is analyzing the association between the pixels or voxels with one another through a series of mathematical methods. The characteristic changes on the medical imaging can reflect the patho-

logical change and histological situation of the organism to some extent. Thus, TA has a unique value in the diagnosis and prognosis prediction of diseases and has gained considerable academic attention. With percutaneous biopsy being the gold standard for diagnostic confirmation, normal imaging technologies such as contrast-enhanced CT and MRI are not satisfying enough and interobserver variability also plays a part in this conundrum, which calls for a new, non-invasive, more accurate technology, since not every patient is willing to perform a biopsy for a small renal mass.[13-15] Furthermore, since enough tissue obtained from the biopsy sample is of great importance in diagnosis, this technique will guide the puncture biopsy by pinpointing the puncture site precisely to improve positive rate.

Therefore, we performed this study to find out the diagnostic accuracy of TA in differentiating RCC and renal lymphoma, further to guide the clinical treatment as well as more accurate puncture biopsy process.

Materials and methods

Patients

From December 2013 to December 2017, 20 renal lymphoma patients from our hospital (West China Hospital, Sichuan University, Chengdu, China) in total meeting our inclusion criteria, which were: 1) lymphoma diagnosed with biopsy/surgery pathological results by the professional pathologists in our institute according to NCCN Guidelines; 2) preoperative ^{18}F-FDG PET/CT results, sufficient follow-up data were available. Patients with past or synchronous other malignant diseases or those who received any kind of treatment before were ruled out from our cohort. Eighteen patients with RCC were chosen to form another group serving as the control group. The complete flow chart of our patient selection process was shown in Figure 1. Our study protocols accord with the Declaration of Helsinki (2013) of the World Medical Association and are approved by the Ethics Committee of West China Hospital of Sichuan University.

Image acquisition and TA

All the ^{18}F-FDG PET/CT scans of our study cohort were performed at our hospital, using a Gemini GXL PET/CT scanner equipped with a 16-slice CT (Philips Medical System, Cleveland, OH, USA). Original images were retrieved from the picture archiving and communication system (PACS) of our electrical history system. We uniformly used 5.0-mm slice CT images and image processing was mainly in cross-sections.

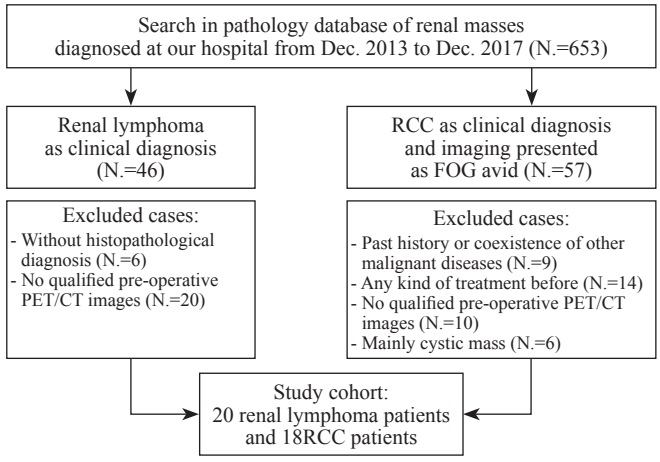

Figure 1.—Flow chart of our patient selection process.

Segmentation

In the identification of volume-of-interest (VOI), we chose to manually draw the region with 3D drawing tool in order to create a representative region. To be specific, we contoured a complete margin of the tumor lesion at all the slices where the lesions can be recognized. Metastatic lesions and inflammatory reaction lesions were excluded.

Radiomic index calculation

Then we used Lifex package, a commercially available software (version 4.00, www.lifexsoft.org), as the tool for calculation of a broad range of conventional, textural and shape indices PET/CT images. Fifty PET and CT radiomics statistics in total, reflecting the VOI shape, the VOI voxel values, the histogram of VOI values, or the VOI textural content, were presented in the form of spreadsheet.[16]

Two experienced radiologists evaluate the PET/CT scans of each patient and give their diagnosis independently as the subjective parameters. Furthermore, they were both blind to the histologic and pathologic results of each patient.

Statistical analysis

Parameters provided by Lifex could be separated into 45 parameters and eight sections, namely Conventional (CONV), Histogram (HISTO), Shape (SHAPE), PARAMS, Grey-Level Co-occurrence Matrix (GLCM), Grey-Level Run Length Matrix (GLRLM), Neighborhood Grey-Level Different Matrix (NGLDM), and Grey-Level Zone Length Matrix (GLZLM). Receiver operating characteristic (ROC) curve was used to examine each parameter. Data like area under the curve (AUC), cut-off value, sensitivity and speci-

ficity were extracted from the analysis output. Binary logistic regression model was used to calculate a joint linear equation for each section and in total. These integrated parameters were then put into ROC analysis again to demonstrate a new set of AUC, cut-off value, sensitivity and specificity values. Chi square test were applied in the baseline information comparison between RCC group and renal lymphoma group. Numerical factors were presented as median and interquartile range (IQR), and categorical factors were presented as frequency and percentage. ROC analysis was processed with MedCalc v. 18.5. Binary logistic regression and Chi square test was done with SPSS v. 25.0.

Results

Patient median ages of RCC and renal lymphoma were 62 and 56, respectively (P=0.492). Nevertheless, we did find a statistically important difference in patient gender (P=0.013), which could be explained by the sex distribution of RCC as well as renal lymphoma, epidemiologically. The complete patient characteristics were displayed in Table I. Figure 2 depicted the PET/CT images of a representative RCC patient and renal lymphoma patient.

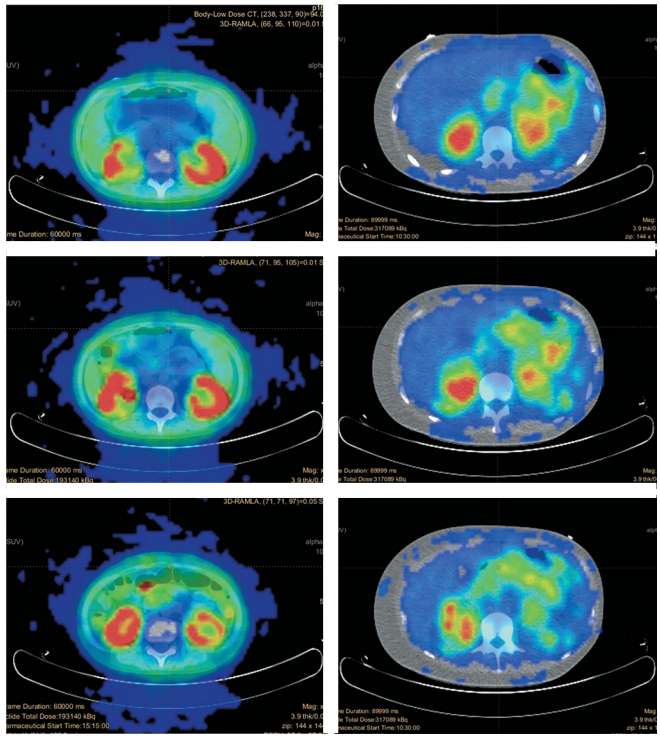

Figure 2.—Comparison of PET/CT images of a representative RCC patient and a renal lymphoma patient.

Median value of conventional PET parameters of the cohort was shown in Table II, and there was no statistically significant difference between RCC group and lymphoma group. A total of 14 texture parameters presented with AUC>0.7 (P<0.05). In detail, these 14 parameters belonged to: HISTO (2; Kurtosis [AUC=0.719, P=0.021], Energy [AUC=0.750, P=0.009]), GLCM (2; Homogeneity [AUC=0.850, P<0.0001], Energy [AUC=0.731, P=0.015]), GLRLM (5; LRE [AUC=0.786, P=0.003], LGRE [AUC=0.850, P<0.0001], SRLGE [AUC=0.844, P<0.0001], LRLGE [AUC=0.858, P<0.0001], GLNU [AUC=0.733, P=0.014]), GLZLM (5; LZE [AUC=0.842, P<0.0001], LGZE [AUC=0.839, P<0.0001], SZLGE [AUC=0.819, P=0.001], LZLGE [AUC=0.853, P<0.0001], LZHGE [AUC=0.708, P=0.028)] sections. Complete data in the ROC analysis of each parameter were shown in Table III.

Since each parameter depicted a single aspect or image

TABLE I.—*Baseline characteristics of patients.*

Characteristics	Total (N.=38)	RCC (N.=18)	Lymphoma (N.=20)	P value
Age				
Median (IQR), years	62.00 (47.75, 66.00)	62.00 (52.50, 67.00)	56.00 (43.25, 64.00)	0.492
<60 years	17	7	10	–
≥60 years	21	11	10	–
Gender	–	–	–	0.013
Male	25	17	8	–
Female	13	1	12	–
Pathological type				
DLBCL	–	–	20	–
Clear cell carcinoma	–	15	–	–
Papillary carcinoma	–	1	–	–
Collecting duct	–	2	–	–
Median tumor volume, mL	51.89 (9.61, 186.31)	54.12 (21.39, 131.85)	38.23 (5.16, 206.86)	

RCC: renal cell carcinoma; DLBCL: diffuse large B-cell lymphoma.

TABLE II.—*Median values of conventional PET parameters and differences between RCC and lymphoma.*

Parameter	Median (IQR)			P value	Standard error difference	95% CI
	Total	RCC	Lymphoma			
SUV_{min}	1.90 (0.92, 2.69)	0.91 (0.60, 1.73)	2.39 (1.96, 2.96)	0.276	8.9683	-29.0243, 8.8166
SUV_{mean}	4.58 (2.37, 7.85)	2.34 (1.9, 4.8)	6.95 (4.35, 9.84)	0.066	1.6835	-6.6054, .2233
SUV_{max}	9.00 (4.83, 15.19)	4.69 (3.35, 11.14)	12.30 (7.64, 17.44)	0.410	41.7501	-52.8293, 123.2855
TLG, mL	166.87 (46.33, 612.82)	166.87 (72.00, 559.40)	244.44 (28.23, 2262.309)	0.049	508.7199	-2127.1030, -5.4581

SUV: standardized uptake value; TLG: total lesion glycolysis; RCC: renal cell carcinoma.

TABLE III.—*ROC analysis results of each single texture features in PET/CT images for RCC* versus *lymphoma.*

Feature	Indices	Sensitivity	Specificity	Cut-off	AUC	P value
CONV	SUV_{min}	0.056	1.000	4.450	0.119	0.000
	SUV_{mean}	0.056	1.000	22.758	0.167	0.000
	SUV_{max}	0.056	1.000	396.584	0.256	0.010
	TLG, mL	0.889	0.350	41.962	0.444	0.559
HISTO	Skewness	0.333	1.000	0.9538	0.603	0.279
	Kurtosis	0.444	0.950	3.6147	0.719	0.021
	Entropy_log10	0.056	0.950	1.5540	0.203	0.002
	Energy	0.556	0.950	0.1390	0.750	0.009
SHAPE	Volume, mL	0.889	0.400	11.32323	0.574	0.438
	Sphericity	0.667	0.600	0.9692	0.614	0.231
	Compacity	0.944	0.400	1.1472	0.586	0.365
PARAMS	Z spatial resampling	0.667	0.400	3.984	0.400	0.293
	Y spatial resampling	1.000	0.000	0.172	0.472	0.770
	X spatial resampling	1.000	0.000	0.172	0.472	0.770
GLCM	Homogeneity	0.778	0.900	0.44925	0.850	0.000
	Energy	0.556	0.900	0.03587	0.731	0.015
	Contrast	1.000	0.100	0.41513	0.261	0.012
	Correlation	1.000	0.35	0.42746	0.658	0.096
	Entropy_log10	1.000	0.100	0.5666	0.308	0.044
	Dissimilarity	1.000	0.100	0.29621	0.228	0.004
GLRLM	SRE	1.000	0.100	0.34281	0.239	0.006
	LRE	0.722	0.850	1.6431	0.786	0.003
	LGRE	0.722	1.000	0.00832	0.850	0.000
	HGRE	1.000	0.100	16.705	0.256	0.010
	SRLGE	0.722	0.95	0.00740	0.844	0.000
	SRHGE	0.111	1.000	1943.600	0.258	0.011
	LRLGE	0.722	1.000	0.01247	0.858	0.000
	LRHGE	1.000	0.100	47.332	0.272	0.017
	GLNU	0.778	0.700	59.833	0.733	0.014
	RLNU	0.944	0.300	77.943	0.544	0.640
	RP	1.000	0.15	0.58557	0.292	0.028
NGLDM	Coarseness	0.944	0.350	0.00225	0.539	0.682
	Contrast	1.000	0.100	0.00544	0.211	0.002
	Busyness	1.000	0.450	0.021	0.539	0.682
GLZLM	SZE	1.000	0.100	0.08102	0.239	0.006
	LZE	0.778	0.800	187.5207	0.842	0.000
	LGZE	0.667	1.000	0.00947	0.839	0.000
	HGZE	0.111	1.000	1882.872	0.289	0.026
	SZLGE	0.611	0.950	0.00452	0.819	0.001
	SZHGE	1.000	0.100	3.524	0.289	0.026
	LZLGE	0.722	1.000	4.539	0.853	0.000
	LZHGE	0.944	0.500	6868.835	0.708	0.028
	GLNU	0.833	0.400	3.448	0.458	0.661
	ZLNU	1.000	0.100	0.500	0.311	0.047
	ZP	1.000	0.100	0.00818	0.203	0.002

RCC: renal cell carcinoma.

TABLE IV.—*ROC analysis results of synthetic texture parameters in PET/CT images for RCC* versus *lymphoma.*

Features	Sensitivity	Specificity	Cut-off	AUC	P value
HISTO	0.778	0.900	0.5471	0.872	<0.0001
SHAPE	1.000	0.500	0.3551	0.725	0.018
PARAMS	1.000	0.350	0.4550	0.600	0.293
GLCM	0.833	0.950	0.4602	0.928	<0.0001
GLRLM	1.000	1.000	0.0007	1.000	<0.0001
NGLDM	0.833	0.800	0.5626	0.817	0.001
GLZLM	0.944	0.950	0.2804	0.975	<0.0001
TOTAL	1.000	1.000	0	1.000	<0.0001

RCC: renal cell carcinoma.

pattern, it was highly specific while not able to describe the whole characteristics of the image. Given the fact mentioned above, each section was combined to create a new variable by binary logistic regression model. These new variables were renamed as HISTO, SHAPE, PARAMS, GLCM, GLRLM, NGLDM and GLZLM. ROC analysis was also performed on them and the results were shown in Table IV. We could see that all of these new parameters demonstrated high AUCs and statistical significance except for PARAMS. To note, the AUCs of GLCM, GLRLM and GLZLM were especially high (0.928, 1.000, 2.975, respectively). Figure 3 exhibited the ROC curves of synthetic parameters.

Discussion

Texture can be comprehended as a resourcefully visual information database, or a "a similarity grouping in an image."[17] In short, texture is certain visual characteristics that reflect the intra-tumor heterogeneity using information contained in the images. Being a fundamental component of postprocessing techniques, TA provides us a new perspective to look at the images and graphics, which contain not only visual information, but also massive amounts of actual, mineable data.[18]

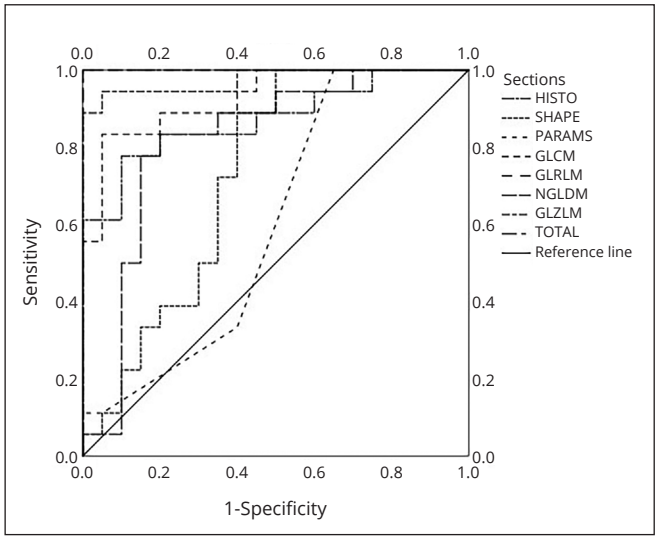

Figure 3.—ROC curves for synthetic texture parameters (HISTO, GLCM, GLRLM, GLZLM, and in total).

Duddalwar *et al*. found that TA shows value in differentiating cRCC from oncocytomas.[19] And experimental results from Kunapuli also demonstrated that radiomics-based features including texture analysis was useful in the clinical decision support.[20] In addition, Skogen *et al*. reported their recognition of applying magnetic resonance imaging texture analysis (MRTA) on discriminating glioblastoma and single brain metastasis.[21] Reports like these certified the effectiveness of TA in differential diagnosis, while still leaving a question mark in the area of RCC versus renal lymphoma specifically. To our knowledge, there are no researches specifically aiming at the differentiation of RCC and renal lymphoma using texture analysis technology based on ^{18}F-FDG PET/CT, thus we have few peer results to compare with.

In this study, we found that there were 14 parameters that belonged to four sections in total presenting a rather good diagnostic potential. Furthermore, it is noteworthy to mention that the diagnostic value of our synthetic texture parameter showed an astounding high AUC, sensitivity and specificity (1.000, 100.00%, 100.00%). For clear cell carcinoma, CEUS and contrast CT show sensitivity values as 94.4% and 88.9%, and specificity values as 45.5% and 72.7%, respectively.[22] Another study reported that, for definite classification of renal masses, sensitivity and specificity of the lesions were 93.8% and 68.4% for MDCT and 93.8% and 71.4% for MRI.[23] We can preliminarily observe that synthetic texture parameter shows a slightly lower sensitivity but a rather higher specificity compared to traditional CEUS, CT and MRI. A 2017 study by Marin *et al*. focused on using contrast-enhanced dual-energy CT with material attenuation analysis to decrease false positive rates of conventional measurements,[24] which indicated that the specificity of these imaging methods were not good enough and more breakthroughs to improve it. ^{18}F-FDG PET/CT has been believed to display its advantages in the preoperative evaluation and staging of metastatic diseases. In bone metastases, it even showed an 100% sensitivity, which raised the problem of false positives. In response to this, our study outcome showed a fairly satisfying direction. TA is a post-processing technology, by using computer language, it can perform data operations

at different levels in single-pixel grayscale in order to provide more imaging information on the basis of traditional imaging methods. Also, high-throughput and quantitative methods are used to mine the information that is easily ignored by the naked eye. Consequently, it can improve the accuracy of artificial diagnosis based on macroscopic image identification.

The SUV metrics (CONVENTIONAL section) did not show a significant difference in our analysis, in line with the results of Nakhoda *et al.*[25] and Kumar *et al*.[26] Findings on this aspect were controversy, however. In 2010, Ye *et al*. compared the mean standardized uptake values and calculated SUVs of renal lymphoma (12 patients, 6.37±2.28 [3.0±13.3]) and RCC (12 patients, 6.27±1.15 [4.2±7.2]).[27] Another study conducted by Nicolau *et al*. in this year included 36 patients (22 were RCCs and 14 were renal lymphomas), and they found that the differences in SUV metrics were statistically important ($P<0.0001$). HISTO, GLCM, GLRLM and GLZLM — these four sections all show high discriminating power in ROC analysis. HISTO and SHAPE belong to the first order features, with HISTO describing the distribution of each pixel in an image, that is, a statistical graph of pixels. GLRLM and GLZLM refers to the size of homogeneous runs or zones for each grey level respectively. GLCM is a cogent texture descriptor by calculating the frequency of pixel pairs appears in an image.[28]

Since the current imaging technologies are not efficient enough in differentiating various histological types, surgical removal of the lesions is inevitably the main modality to treat these diseases, even though it may not be the most appropriate option for each one of these subtypes. For instance, even if there are currently no standard recommendation for renal lymphoma patients, some long-time follow-up studies hold the belief that systemic chemotherapy or combination chemotherapy supplemented by surgery may be a better option for renal lymphoma instead of merely radical nephrectomy.[29] Consequently, it is of significance to develop a new standard or methodology to effectively identify some of these subtypes which are not suitable for radical nephrectomy such as renal lymphoma with high sensitivity and accuracy. When renal lymphoma presents as a solitary nodule, radiologists often rely on some circumstantial evidence like retroperitoneal lymphadenopathy, splenomegaly, tumor thrombus, central necrotic region. Therefore, it is not easy to differentiate it from RCC.[13, 14, 22] We can say that the identification of RCC and renal lymphoma remains a diagnostic challenge for radiologists and clinicians.

Our findings revealed that the texture parameters of PET/CT could be of use in assisting the differentiation of RCC and renal lymphoma. As far as we know, no study on the differential diagnosis of RCC with renal lymphoma has been reported yet, which makes us the first to look into this area. The authors think that, due to its quantifiable nature, applying TA on image data will benefit the clinical decision-making process. Not only can TA be an instructive guidance during the biopsy, it has the potential to develop higher diagnostic value as a noninvasive method. At the meantime, the TA information of each patient can provide more detailed and personalized treatment advice, by comparing the TA result of the patient's imaging examinations at different times. Of course, larger and prospective researches are needed in order to accomplish this transfer from artificially visual-recognition pattern to data-analyzing imaging, and histology or biopsy confirmation is still needed in this phase for clinical therapeutic decision. We hope that future studies will validate our findings in not only renal masses but also other malignancies to extend the application of TA. Also, the influence, or to say predictive value of TA on the prognosis of patients with various renal masses should be discussed in the future. Further, from a more technical point of view, we would like to pay more attention to the combination of computer science and clinical imaging area, in order to figure out the mechanisms behind.

Limitations of the study

There are a few limitations we need to put forward. Our study population is not very large and the diagnosis time is limited to recent years. We are aware that this may present a negative effect on detecting the consistency of diagnostic method. However, lymphomas involving kidneys, no matter if they are a comorbidity of systemic malignancy or primary renal lymphoma, are not commonly seen, especially the latter one, which has only been discussed in case reports to our knowledge.[30, 31] Also, this is a retrospective single-institute study, which has its inherit disadvantages. In addition, the pathological subtypes of our cohort database are relatively small for both RCC and renal lymphoma. The benefit is that we can better focus on the specific subtype and explore more detail about it, while in the meantime the disadvantages being that we cannot provide a full understanding of the whole histological influence.

Conclusions

The application of TA enables us to explore the relationship between clinicopathology and the survival prognosis

of patients by mining and processing vast amounts of information. In this study, we firstly report the clinical significance of TA of ^{18}F-FDG PET/CT within RCC and renal lymphoma patients. Future studies in wider disease range and into more specific mechanism will be needed.

References

1. Campbell S, Uzzo RG, Allaf ME, Bass EB, Cadeddu JA, Chang A, *et al.* Renal Mass and Localized Renal Cancer: AUA Guideline. J Urol 2017;198:520–9.

2. Berland LL, Silverman SG, Gore RM, Mayo-Smith WW, Megibow AJ, Yee J, *et al.* Managing incidental findings on abdominal CT: white paper of the ACR incidental findings committee. J Am Coll Radiol 2010;7:754–73.

3. Lipworth L, Tarone RE, McLaughlin JK. The epidemiology of renal cell carcinoma. J Urol 2006;176:2353–8.

4. MacLennan S, Imamura M, Lapitan MC, Omar MI, Lam TB, Hilvano-Cabungcal AM, *et al.*; UCAN Systematic Review Reference Group; EAU Renal Cancer Guideline Panel. Systematic review of perioperative and quality-of-life outcomes following surgical management of localised renal cancer. Eur Urol 2012;62:1097–117.

5. MacLennan S, Imamura M, Lapitan MC, Omar MI, Lam TB, Hilvano-Cabungcal AM, *et al.*; UCAN Systematic Review Reference Group; EAU Renal Cancer Guideline Panel. Systematic review of oncological outcomes following surgical management of localised renal cancer. Eur Urol 2012;61:972–93.

6. Ballonoff A, Rusthoven KE, Schwer A, McCammon R, Kavanagh B, Bassetti M, *et al.* Outcomes and effect of radiotherapy in patients with stage I or II diffuse large B-cell lymphoma: a surveillance, epidemiology, and end results analysis. Int J Radiat Oncol Biol Phys 2008;72:1465–71.

7. Pfreundschuh M, Trümper L, Osterborg A, Pettengell R, Trneny M, Imrie K, *et al.*; MabThera International Trial Group. CHOP-like chemotherapy plus rituximab versus CHOP-like chemotherapy alone in young patients with good-prognosis diffuse large-B-cell lymphoma: a randomised controlled trial by the MabThera International Trial (MInT) Group. Lancet Oncol 2006;7:379–91.

8. Rohlfing S, Dietrich S, Witzens-Harig M, Hegenbart U, Schönland S, Luft T, *et al.* The impact of stem cell transplantation on the natural course of peripheral T-cell lymphoma: a real-world experience. Ann Hematol 2018;97:1241–50.

9. Luciano RL, Brewster UC. Kidney involvement in leukemia and lymphoma. Adv Chronic Kidney Dis 2014;21:27–35.

10. Samlowski EE, Dechet C, Weissman A, Samlowski WE. Large cell non-Hodgkin's lymphoma masquerading as renal carcinoma with inferior vena cava thrombosis: a case report. J Med Case Reports 2011;5:245.

11. Tefekli A, Baykal M, Binbay M, Barut M, Muslumanoglu AY. Lymphoma of the kidney: primary or initial manifestation of rapidly progressive systemic disease? Int Urol Nephrol 2006;38:775–8.

12. Alic L, Niessen WJ, Veenland JF. Quantification of heterogeneity as a biomarker in tumor imaging: a systematic review. PLoS One 2014;9:e110300.

13. Pedrosa I, Sun MR, Spencer M, Genega EM, Olumi AF, Dewolf WC, *et al.* MR imaging of renal masses: correlation with findings at surgery and pathologic analysis. Radiographics 2008;28:985–1003.

14. Urban BA, Fishman EK. Renal lymphoma: CT patterns with emphasis on helical CT. Radiographics 2000;20:197–212.

15. Sheth S, Ali S, Fishman E. Imaging of renal lymphoma: patterns of disease with pathologic correlation. Radiographics 2006;26:1151–68.

16. Nioche C, Orlhac F, Boughdad S, Reuzé S, Goya-Outi J, Robert C, *et al.* LIFEx: A Freeware for Radiomic Feature Calculation in Multimodality Imaging to Accelerate Advances in the Characterization of Tumor Heterogeneity. Cancer Res 2018;78:4786–9.

17. Serra J. Image Analysis and Mathematical Morphology. London: Academic Press, Inc.; 1983.

18. Gillies RJ, Kinahan PE, Hricak H. Radiomics: Images Are More than Pictures, They Are Data. Radiology 2016;278:563–77.

19. Duddalwar V, Zhang X, Hwang D, Cen S, Yap F, Ugwueze C, *et al.* PD14-07 differentiation between clear cell renal cell carcinomas and oncocytomas using texture analysis of CT images. J Urol 2016;195:e305.

20. Kunapuli G, Varghese BA, Ganapathy P, Desai B, Cen S, Aron M, *et al.* A Decision-Support Tool for Renal Mass Classification. J Digit Imaging 2018;31:929–39.

21. Skogen K, Schulz A, Helseth E, Ganeshan B, Dormagen JB, Server A. Texture analysis on diffusion tensor imaging: discriminating glioblastoma from single brain metastasis. Acta Radiol 2019;60:356–66.

22. Tamai H, Takiguchi Y, Oka M, Shingaki N, Enomoto S, Shiraki T, *et al.* Contrast-enhanced ultrasonography in the diagnosis of solid renal tumors. J Ultrasound Med 2005;24:1635–40.

23. Beer AJ, Dobritz M, Zantl N, Weirich G, Stollfuss J, Rummeny EJ. Comparison of 16-MDCT and MRI for characterization of kidney lesions. AJR Am J Roentgenol 2006;186:1639–50.

24. Marin D, Davis D, Roy Choudhury K, Patel B, Gupta RT, Mileto A, *et al.* Characterization of Small Focal Renal Lesions: Diagnostic Accuracy with Single-Phase Contrast-enhanced Dual-Energy CT with Material Attenuation Analysis Compared with Conventional Attenuation Measurements. Radiology 2017;284:737–47.

25. Nakhoda Z, Torigian DA, Saboury B, Hofheinz F, Alavi A. Assessment of the diagnostic performance of (18)F-FDG-PET/CT for detection and characterization of solid renal malignancies. Hell J Nucl Med 2013;16:19–24.

26. Kumar R, Chauhan A, Lakhani P, Xiu Y, Zhuang H, Alavi A. 2-Deoxy-2-[F-18]fluoro-D-glucose-positron emission tomography in characterization of solid renal masses. Mol Imaging Biol 2005;7:431–9.

27. Ye XH, Chen LH, Wu HB, Feng J, Zhou WL, Yang RM, *et al.* 18F-FDG PET/CT evaluation of lymphoma with renal involvement: comparison with renal carcinoma. South Med J 2010;103:642–9.

28. Nicolau C, Sala E, Kumar A, Goldman DA, Schoder H, Hricak H, *et al.* Renal Masses Detected on FDG PET/CT in Patients With Lymphoma: Imaging Features Differentiating Primary Renal Cell Carcinomas From Renal Lymphomatous Involvement. AJR Am J Roentgenol 2017;208:849–53.

29. Vázquez-Alonso F, Puche-Sanz I, Sánchez-Ramos C, Flores-Martín J, Vicente-Prados J, Cózar-Olmo JM. Primary renal lymphoma: long-term results of two patients treated with a chemotherapy + rituximab protocol. Case Rep Oncol Med 2012;2012:726424.

30. Ladha A, Haider G. Primary renal lymphoma. J Coll Physicians Surg Pak 2008;18:584–5.

31. Omer HA, Hussein MR. Primary renal lymphoma. Nephrology (Carlton) 2007;12:314–5.

Conflicts of interest.—The authors certify that there is no conflict of interest with any financial organization regarding the material discussed in the manuscript.

Authors' contributions.—Sha Zhu, Hui Xu, and Xuelei Ma contributed equally to this work. Sha Zhu: manuscript writing/editing; protocol/project development. Hui Xu, Xuelei Ma: protocol/project development. Chuyu Shen, Yingjie Wang, Wenting Xu: data collection or management. Shihao Duan, Hanxiao Chen: data analysis. Xuejin Ou, Linyan Chen: data analysis; data collection or management.

History.—Article first published online: May 27, 2019. - Manuscript accepted: May 22, 2019. - Manuscript revised: April 3, 2019. - Manuscript received: September 27, 2018.